

# CRISPR-MiX: A pooled single-stranded donor strategy to enhance HDR efficiency in human iPSCs

Rachel Baum,<sup>1,2</sup> Narasimha Telugu,<sup>4</sup> Arne A.N. Bruyneel,<sup>1,2</sup> Maryam Kay,<sup>1,2</sup> Pooja Nair,<sup>1,2</sup> Isaac Perea-Gil,<sup>1,2</sup> Vittavat Termglinchan,<sup>1,2</sup> Nike Bharucha,<sup>1,2</sup> Edina Lee,<sup>1,2</sup> Mark Mercola,<sup>1,2,3</sup> Sebastian Diecke,<sup>4,5</sup> and Ioannis Karakikes<sup>1,2</sup>

<sup>1</sup>Cardiovascular Institute, Stanford University School of Medicine, Stanford, CA 94305, USA; <sup>2</sup>Department of Cardiothoracic Surgery, Stanford University School of Medicine, Stanford, CA 94304, USA; <sup>3</sup>Departments of Medicine, Division of Cardiovascular Medicine, Stanford University, Stanford, CA 94305, USA; <sup>4</sup>Max Delbrück Center for Molecular Medicine (MDC), 13125 Berlin, Germany; <sup>5</sup>DZHK (German Centre for Cardiovascular Research), Partner Site Berlin, 10785 Berlin, Germany

**CRISPR-Cas9 is widely used to model genetic disorders by introducing or correcting disease-associated mutations in induced pluripotent stem cells (iPSCs) through homology-directed repair (HDR). However, HDR efficiency in iPSCs remains low and is highly dependent on the target locus. Here, we developed CRISPR-MiX, an improved protocol to enhance HDR efficiency in human iPSCs. Using a GFP-to-BFP reporter system, we identified key single-stranded oligodeoxynucleotide (ssODN) donor design parameters, including homology arm symmetry, CRISPR/Cas-blocking mutations, and strand complementarity, which significantly influence HDR outcomes. We applied this approach to introduce pathogenic variants into five genes related to genetic cardiomyopathies. Quantitative analysis of HDR events showed that both the target locus and ssODN design strongly affect HDR efficiency. To address the locus- and design-specific limitations, we established CRISPR-MiX, a pooled ssODN-based method for scarless genome editing using ribonucleoproteins (RNPs) that does not require selection. CRISPR-MiX consistently improved HDR efficiency across multiple loci. This strategy offers a simple, robust, and versatile approach for precise genome engineering in iPSCs, supporting broad applications in disease modeling and functional genomics.**

## INTRODUCTION

Many genetic disorders have been modeled *in vitro* by deriving induced pluripotent stem cells (iPSCs) from patients carrying pathogenic mutations. However, somatic cell reprogramming to iPSCs takes several months and is often limited by patient availability. To expedite the process and overcome these challenges, targeted genomic engineering of disease-causing mutations in a reference “wild-type” cell line has been explored as an alternative approach. This method typically requires only a few weeks and provides an isogenic control line for direct comparison. However, modifying iPSCs at specific loci remains challenging and often results in low and variable editing efficiencies.

Genome editing with custom endonuclease relies on two mechanisms of DNA repair: homology-directed repair (HDR) and non-homologous end joining (NHEJ). HDR is preferred for knockin, knockout, or precise mutagenesis, but it is an inefficient process. In the fast-evolving CRISPR/Cas9 genome editing field, substantial efforts have been made to enhance the efficiency of HDR; yet, reported success rates remain variable and relatively low.<sup>1–3</sup>

Strategies to enhance HDR efficiency include inhibiting the NHEJ pathway through chemical and genetic modulation,<sup>4–12</sup> controlling factors such as temperature,<sup>8,9</sup> using Cas9 fusion proteins,<sup>13</sup> or synchronizing the cell cycle.<sup>1,12</sup> However, these approaches are often cell-type- and experimental-conditions-dependent. Microhomology-mediated end joining (MMEJ) is an additional repair pathway that can be utilized to enhance HDR. MMEJ utilizes short homologous sequences to repair double-stranded breaks, and recent work demonstrated that simultaneous inhibition of NHEJ and MMEJ enhanced HDR efficiency.<sup>14</sup>

Another way to enhance HDR efficiency is through the rational design of the homology repair donor templates. Studies have shown that adjusting the lengths of repair template homology regions using asymmetric single-stranded oligodeoxynucleotides (ssODNs) can positively impact editing efficiency.<sup>5,15–17</sup> Additionally, incorporating a silent mutation in the PAM sequence to block the re-cutting of the targeted site<sup>2,18–20</sup> can improve accuracy and efficiency.

---

Received 22 April 2025; accepted 30 December 2025;  
<https://doi.org/10.1016/j.omtn.2025.102820>.

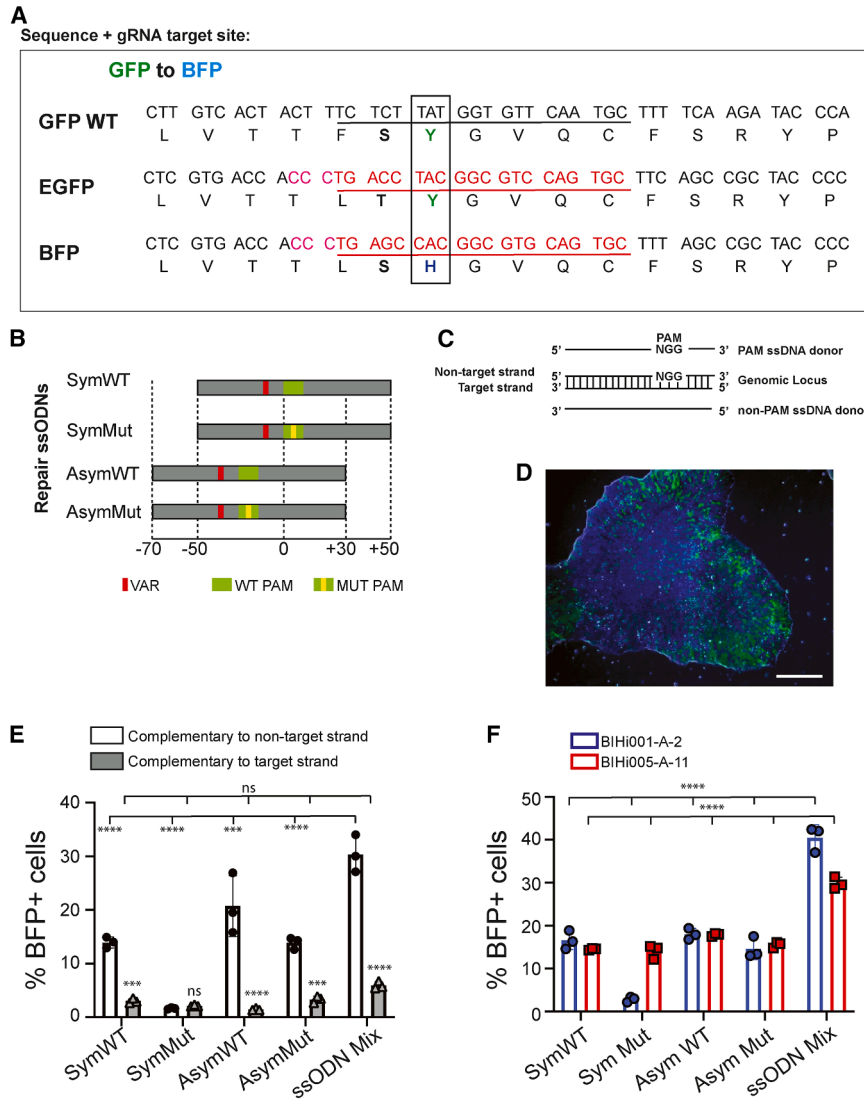
**Correspondence:** Sebastian Diecke, Max Delbrück Center for Molecular Medicine (MDC), 13125 Berlin, Germany.

E-mail: [sebastian.diecke@mdc-berlin.de](mailto:sebastian.diecke@mdc-berlin.de)

**Correspondence:** Ioannis Karakikes, Department of Cardiothoracic Surgery, Stanford University School of Medicine, CA 94305, USA.

E-mail: [ioannis1@stanford.edu](mailto:ioannis1@stanford.edu)





Despite these advancements, achieving efficient HDR in iPSCs remains challenging, with success rates varying by cell type, locus, and experimental conditions. Here, we developed a method, termed “CRISPR-MiX,” to address these challenges. By combining multiple rationally designed ssODNs, CRISPR-MiX enables scarless genome editing with improved HDR efficiency, independent of the locus or donor design.

## RESULTS

### Optimizing ssODN design improves HDR efficiency in iPSCs

Improving HDR efficiency is a key challenge in achieving reliable insertions in iPSCs. Short ssODN donor templates containing a mutation of interest have been used to facilitate HDR-mediated genome editing. To evaluate the HDR efficiency of ssODNs, we utilized an engineered reporter human iPSC line harboring the green fluores-

**Figure 1. ssODN design parameters influence HDR efficiency in a GFP-to-BFP reporter system**

(A) Schematic of the GFP-to-BFP reporter system. The underlined sequence indicates the gRNA target site, and the black box highlights the targeted amino acid substitution (Y66H) that shifts fluorescence from GFP to BFP. (B) Schematic of ssODN designs showing homology arm symmetry (symmetric vs. asymmetric) and the presence or absence of a PAM-blocking mutation (WT vs. Mut). (C) Schematic illustrating complementarity to either the non-target or the target DNA strand. (D) Representative fluorescence images of iPSCs showing GFP- and BFP-positive cells following genome editing. Scale bars, 200  $\mu$ m. (E) Quantification of the percentage of BFP-positive cells in the homozygous AAVS1-GFP reporter iPSC line (BIHi001-A-2). Student’s *t* test comparing target to the non-target strand within each ssODN group (\**p* < 0.05, \*\**p* < 0.01, \*\*\**p* < 0.001, \*\*\*\**p* < 0.0001); two-way ANOVA with Tukey’s multiple comparisons test comparing ssODN mix vs. individual designs within each strand group (\*\*\*\**p* < 0.0001; ns, not significant). Data are presented as mean  $\pm$  SD, *n* = 3 independent experiments per group. (F) Quantification of BFP-positive cells across two reporter lines (BIHi001-A-2 and BIHi005-A-11). Two-way ANOVA with Tukey’s multiple comparisons test comparing ssODN mix vs. individual designs within each cell line (\*\*\*\**p* < 0.0001). No significant differences were observed between cell lines by one-way ANOVA. Data are presented as mean  $\pm$  SD, *n* = 3 independent experiments per group.

cent protein (GFP) to blue fluorescent protein (BFP) conversion system.<sup>21</sup>

The reporter cells express the GFP protein, but a nucleotide substitution (196T>C) converts the tyrosine amino acid to histidine (Y66H), shifting the fluorescence excitation and emission spectra from GFP to BFP (Figure 1A). This reporter system allows for precise measurement of HDR efficiency by quantifying the percentage of cells that shift from GFP to BFP.

To test whether the design of the ssODN affects HDR efficiency in the GFP-to-BFP iPSC reporter line (BIHi001-A-2; <https://hpscreg.eu/cell-line/BIHi001-A-2>; Homozygous AAVS1-GFP), we created eight ssODNs with variable homology arm length (5' or 3' symmetry), the presence of a blocking mutation in the PAM sequence (Figure 1B), and strand complementary (Figure 1C; Tables S1 and S2). Using nucleofection, we delivered pre-assembled Cas9 ribonuclease (RNP) complexes along with the ssODNs to the iPSC reporter line. Each of the four ssODNs was delivered either individually or as a pool in equimolar ratios (1:1:1, “CRISPR-MiX”). We assessed HDR by measuring the conversion of GFP to BFP using fluorescence-activated cell sorting (FACS) analysis and quantified the percentage of BFP-positive cells (Figures 1D, 1E, and S1A).

We observed HDR efficiencies (GFP-to-BFP conversion) ranging from 2% to 20%, depending on the ssODN design (Figure 1E). We found that symmetric and asymmetric donors stimulated HDR at similar frequencies. Consistent with previous studies,<sup>22</sup> we also observed significantly higher GFP-to-BFP conversion rates when the donor DNA was complementary to the non-target strand (Figure 1E). Importantly, we observed a significantly higher GFP-to-BFP conversion in the pooled ssODN group than in any individual ssODN, outperforming the best individual ssODN (AsymWT).

To corroborate these findings and rule out allele-specific effects, we repeated the experiments in a heterozygous Oct4-GFP knockin iPSC line (B1Hi005-A-11; Oct4-GFP (<https://hpscreg.eu/cell-line/B1Hi005-A-11>) in which the GFP is expressed in the endogenous POUF51 locus. We utilized this cell line to evaluate HDR at a single allele within a transcriptionally active locus. Similar to the homozygous AAVS1-GFP reporter, we observed variability in HDR with single ssODN donor templates, whereas pooling significantly increased HDR (Figures 1F and S1). In contrast, adding a PAM-blocking substitution in the homozygous AAVS1-GFP reporter was associated with decreased HDR for both the symmetric and, to a lesser extent, the asymmetric donor; this effect was not observed in the heterozygous POUF51-GFP line (Figures 1F and S1).

Together, results confirm that HDR efficiency depends on the ssODN design in both homozygous and heterozygous reporter lines and show that pooling donor templates enhances editing outcomes across different genomic contexts.

#### CRISPR-MiX enables efficient genome editing across cardiomyopathy genes

Next, we sought to evaluate the efficiency of ssODN donor templates to introduce disease-causing mutations in a reference “wild-type” iPSC line. To simulate a practical use experiment, we targeted five endogenous loci to introduce mutations in genes associated with familial cardiomyopathies, including phospholamban (PLN, p.R14del),<sup>23,24</sup> tropomyosin (TPM1, p.E39K),<sup>25</sup> cardiac troponin T (TNNT2, p.R183W),<sup>26</sup> RNA-binding motif protein 20 (RBM20, p.R636Q),<sup>27</sup> and potassium voltage-gated channel subfamily H member 2 (KCNH2, p.T983I)<sup>28</sup> (Figures 2A and S2). Each locus was targeted with Cas9-gRNA RNP (Table S3) and ssODNs (Tables S1 and S2), delivered by electroporation to the iPSCs, and HDR was quantified by amplicon sequencing in unselected iPSCs.<sup>27</sup>

We observed HDR events in all five loci (Figure 2B) using the non-target strand individual ssODN designs; however, HDR efficiencies varied among the targeted loci (range, 0.1%–6%), depending on the design (Figure 2C). Furthermore, the most efficient ssODN design differed across different loci (Figure 2C). For example, at the PLN locus, the asymmetric donor ssODN with a PAM-blocking mutation (AsymMut) yielded the highest HDR ( $4.94\% \pm 0.035\%$ ). In contrast, at the TPM1 locus, the symmetric ssODN donor without the PAM-blocking mutation (SymWT) achieved the highest HDR

efficiency ( $6.195\% \pm 0.033\%$ ). These data suggest that each genomic locus may have an inherent preference for ssODN donor template design. In contrast, CRISPR-MiX produced consistent HDR across all five loci, with HDR significantly higher than that of any single donor at TNNT2, KCNH2, RBM20, and TPM1 ( $p < 0.05$ ). At PLN, CRISPR-MiX was comparable to the best single design (AsymMut) but exceeded AsymWT, SymWT, and SymMut ( $p \leq 0.0016$ ).

To evaluate strand-specific effects, we also examined CRISPR-MiX-mediated HDR using ssODNs derived from the target DNA strand. HDR was highly dependent on the locus and ssODN design (Figure 2D). Compared to the non-target strand, the target strand CRISPR-MiX performed similarly at the PLN and TPM1 loci and was more effective at the TNNT2 locus. However, neither the individual donors nor the CRISPR-MiX of pooled donors showed any successful HDR at KCNH2 or RBM20.

#### DISCUSSION

CRISPR/Cas9 genome editing is a powerful tool for introducing and correcting genetic mutations in human iPSCs. However, CRISPR/Cas9-mediated HDR often has low success rates. Although strategies to improve HDR have been developed, results depend on the template design and the targeted locus. By systematically testing variables including strand complementarity, homology arm symmetry, and the presence of PAM-blocking mutations, we developed “CRISPR-MiX,” a pooled ssODN approach that consistently achieves HDR across multiple loci, enabling efficient CRISPR/Cas9-mediated genome editing in human iPSCs.

Across the tested conditions, strand orientation emerged as a critical determinant of HDR-mediated genome editing. Donors complementary to the non-target strand generally produced higher or more consistent HDR than target-strand donors, although the magnitude and direction of this effect depended on experimental context. Including the Cas9 variant used,<sup>22</sup> our findings are consistent with prior reports but differ from Skarnes et al. (2019),<sup>29</sup> who reported no strand dependence in a monoallelic AAVS1 BFP-to-GFP reporter. Differences in allelic context, gRNA positioning, and experimental conditions, such as cold shock, ssODN chemical modifications, and small molecule HDR “enhancer,” likely account for these discrepancies. This suggests that strand effects are system-specific, supporting empirical strand testing and pooled donor strategies. Finally, we found that homology-arm symmetry and PAM protection also influenced HDR outcomes, but their effects depended on locus and design, highlighting that donor configuration affects HDR outcomes.

Extending these observations to endogenous targets, we examined five cardiomyopathy-associated genes using both individual donors and pooled CRISPR-MiX on each strand. On the non-target strand, CRISPR-MiX was significantly higher than any single donor at four loci or matched the best single design at the fifth locus. On the target strand, outcomes were strongly locus-dependent: CRISPR-MiX improved HDR at some loci, was comparable to single donors at others,

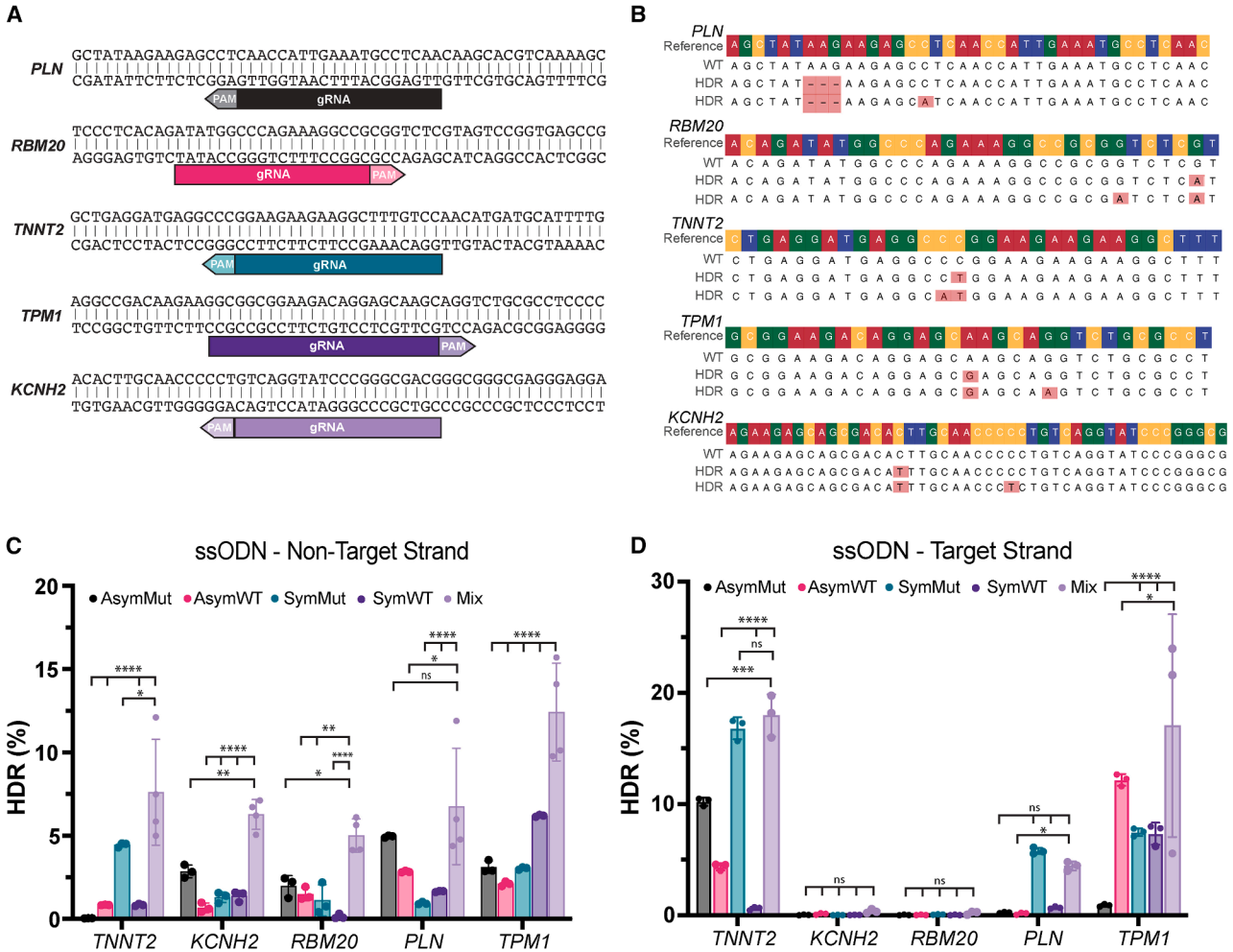


**Figure 2. CRISPR-MiX improves HDR efficiency at endogenous cardiomyopathy-associated loci**

(A) Schematic of sequences at the targeted loci associated with pathogenic cardiomyopathy mutations. (B) Representative amplicon sequencing reads showing the success of HDR at the target loci using AlleleProfileR. (C and D) HDR efficiency (%) calculated by amplicon sequencing for each targeted gene (PLN, TPM1, TNNT2, RBM20, and KCNH2) using individual ssODNs or pooled ssODNs (CRISPR-MiX) targeting either the non-target strand (C) or the target strand (D). Statistical analysis by two-way ANOVA with Dunnett's multiple comparisons (reference = Mix) was performed within each gene. Data are presented as mean  $\pm$  SD,  $n = 3-4$  independent experiments per group (\* $p < 0.05$ , \*\* $p < 0.01$ , \*\*\* $p < 0.001$ , \*\*\*\* $p < 0.0001$ ).

and produced no detectable HDR at loci where target-strand donors failed. These results demonstrate that pooling rationally designed donors, especially those from the non-target DNA strand, reduces locus-specific variability and delivers robust HDR without the need for extensive locus-by-locus optimization. Nevertheless, empirical testing may be required for particular loci to achieve optimal outcomes.

Mechanistically, we postulate that CRISPR-MiX enhances HDR efficiency by increasing compatibility with the diverse DNA repair microenvironments present at different loci and across individual cells. Following Cas9-induced double-strand breaks, repair is initiated via DNA end resection, which can vary in extent and polarity depending on locus-specific features. For example, loci that

undergo minimal or asymmetric resection may more readily anneal to ssODNs of a particular strand or homology arm configuration. This could explain why certain loci (e.g., KCNH2 and RBM20) failed to support HDR with target strand donors, while others (e.g., TNNT2) favored them. By pooling multiple ssODNs with diverse designs, CRISPR-MiX likely increases the chance of donor-resection compatibility, thereby compensating for variability in resection dynamics and chromatin context and overcoming locus-specific repair constraints.

In summary, we developed CRISPR-MiX, a pooled ssODN approach for enhancing HDR in human iPSCs, enabling rapid and predictable genome editing. Although our study focused on iPSCs, the principle of CRISPR-MiX could also be applied to more complex systems, such

as iPSC-derived organoids and primary cells. Given its versatility, CRISPR-MiX holds broad potential in disease modeling, functional genomics, and therapeutic genome engineering.

## MATERIALS AND METHODS

### Human iPSC reprogramming and culture

The human iPSCs were derived from peripheral blood mononuclear cells (PBMCs) using the CytoTune-iPS Sendai Reprogramming Kit (Thermo Fisher Scientific) per the manufacturer's protocol with some modifications, as previously described.<sup>23–26</sup>

The iPSCs were cultured in E8 media on Geltrex-coated plates at 37°C under hypoxic conditions (5% O<sub>2</sub>, 8% CO<sub>2</sub>). Cells were dissociated using DPBS-EDTA at 37°C for 7–10 min and replated in E8 media containing 2.5 μM Y-27632 (Selleckchem).

### Genome editing

Ribonucleoprotein (RNP) complexes were assembled by mixing 60 pmol sgRNA (Synthego; sequences in Table S3) with 20 pmol SpCas9 nuclease (Synthego) and incubating for 10 min at room temperature. Next, for electroporation, 120 pmol of ssODNs was added to the RNP complexes in a total volume of 10 μL in R buffer (Thermo Fisher Scientific). The RNP-ssODN mixture was electroporated into iPSCs (0.25 × 10<sup>6</sup> cells) using the Neon Transfection System (Thermo Fisher Scientific) with a 10μL Neon Tip (1,200 V, 20 ms, 1 pulse).

Following electroporation, the cells were plated in a 6-well plate with E8 medium supplemented with CloneR2 (STEMCELL Technologies). The cells were harvested 5 days post-nucleofection for flow cytometric quantification of BFP, allowing time for the reporter protein expression. The cells were dissociated and analyzed by flow cytometry to quantify GFP and BFP expression using the MACSQuant 10 system (Miltenyi Biotec). The data were analyzed with FlowJo software. For endogenous gene editing assays, genomic DNA was extracted 2 days post-electroporation, a time point sufficient to detect HDR events by amplicon sequencing.

### Amplicon sequencing

Genomic DNA was extracted using QuickExtract solution (Epicenter) following the manufacturer's protocol. The targeted regions were amplified by PCR using the PrimeSTAR GXL DNA Polymerase (Takara) with locus-specific primers (Table S4). PCR products were sequenced using the Amplicon-EZ sequencing service (Genewiz).

### HDR analysis

The HDR analysis was performed using AlleleProfileR by providing the reference genome (hg38), the gRNA sequences, the next-generation sequencing reads, and the amplicon sequences of each target locus, following the software's manual.<sup>27</sup>

## DATA AVAILABILITY

The data of this study are available upon request from the corresponding authors.

## ACKNOWLEDGMENTS

This research was supported by grants from the NIH R01 HL139679 and R01 HL150414 (to I.K.), the Leducq Foundation (to I.K.), F32 and T32 (to R.B.), the AHA fellowship (to I.P.-G.), the German Centre for Cardiovascular Research (DZHK Partner site Berlin), and HORIZON-EIC-2022-PATHFINDERCHALLENGES-01-03 NaV1.5-CARED (to S.D.).

## AUTHOR CONTRIBUTIONS

I.K. conceptualized the project. N.T., A.A.N.B., P.N., I.P.-G., V.T., M.K., and N.B. conducted the experiments. M.M., S.D., and I.K. designed the experiments. R.B., S.D., and I.K. analyzed the data. E.L. created graphical abstracts. R.B., S.D., and I.K. wrote the paper.

## DECLARATION OF INTERESTS

The authors declare no competing interests.

## SUPPLEMENTAL INFORMATION

Supplemental information can be found online at <https://doi.org/10.1016/j.omtn.2025.102820>.

## REFERENCES

- Lin, S., Staahl, B.T., Alla, R.K., and Doudna, J.A. (2014). Enhanced homology-directed human genome engineering by controlled timing of CRISPR/Cas9 delivery. *eLife* 3, e04766.
- Paquet, D., Kwart, D., Chen, A., Sproul, A., Jacob, S., Teo, S., Olsen, K.M., Gregg, A., Noggle, S., and Tessier-Lavigne, M. (2016). Efficient introduction of specific homozygous and heterozygous mutations using CRISPR/Cas9. *Nature* 533, 125–129.
- Takayama, K., Igai, K., Hagiwara, Y., Hashimoto, R., Hanawa, M., Sakuma, T., Tachibana, M., Sakurai, F., Yamamoto, T., and Mizuguchi, H. (2017). Highly efficient biallelic genome editing of human ES/iPS cells using a CRISPR/Cas9 or TALEN system. *Nucleic Acids Res.* 45, 5198–5207.
- Maruyama, T., Dougan, S.K., Truttmann, M.C., Bilate, A.M., Ingram, J.R., and Ploegh, H.L. (2015). Increasing the efficiency of precise genome editing with CRISPR-Cas9 by inhibition of nonhomologous end joining. *Nat. Biotechnol.* 33, 538–542.
- Chu, V.T., Weber, T., Wefers, B., Wurst, W., Sander, S., Rajewsky, K., and Kühn, R. (2015). Increasing the efficiency of homology-directed repair for CRISPR-Cas9-induced precise gene editing in mammalian cells. *Nat. Biotechnol.* 33, 543–548.
- Yu, C., Liu, Y., Ma, T., Liu, K., Xu, S., Zhang, Y., Liu, H., La Russa, M., Xie, M., Ding, S., and Qi, L.S. (2015). Small molecules enhance CRISPR genome editing in pluripotent stem cells. *Cell Stem Cell* 16, 142–147.
- Pinder, J., Salsman, J., and Dellaire, G. (2015). Nuclear domain 'knock-in' screen for the evaluation and identification of small molecule enhancers of CRISPR-based genome editing. *Nucleic Acids Res.* 43, 9379–9392.
- Maurissen, T.L., and Woltjen, K. (2020). Synergistic gene editing in human iPS cells via cell cycle and DNA repair modulation. *Nat. Commun.* 11, 2876.
- Guo, Q., Mintier, G., Ma-Edmonds, M., Storton, D., Wang, X., Xiao, X., Kienzle, B., Zhao, D., and Feder, J.N. (2018). Cold shock increases the frequency of homology directed repair gene editing in induced pluripotent stem cells. *Sci. Rep.* 8, 2080.
- Li, G., Liu, D., Zhang, X., Quan, R., Zhong, C., Mo, J., Huang, Y., Wang, H., Ruan, X., Xu, Z., et al. (2018). Suppressing Ku70/Ku80 expression elevates homology-directed repair efficiency in primary fibroblasts. *Int. J. Biochem. Cell Biol.* 99, 154–160.
- Yu, S., Song, Z., Luo, J., Dai, Y., and Li, N. (2011). Over-expression of RAD51 or RAD54 but not RAD51/4 enhances extra-chromosomal homologous recombination in the human sarcoma (HT-1080) cell line. *J. Biotechnol.* 154, 21–24.
- Yang, D., Scavuzzo, M.A., Chmielowiec, J., Sharp, R., Bajic, A., Borowiak, M., and McMahon, A.P. (2016). Enrichment of G2/M cell cycle phase in human pluripotent stem cells enhances HDR-mediated gene repair with customizable endonucleases. *Sci. Rep.* 6, 21264.
- Charpentier, M., Khedher, A.H.Y., Menoret, S., Brion, A., Lamribet, K., Dardillac, E., Boix, C., Perrouault, L., Tesson, L., Geny, S., et al. (2018). CtIP fusion to Cas9 enhances transgene integration by homology-dependent repair. *Nat. Commun.* 9, 1133.

14. Wimberger, S., Akrap, N., Firth, M., Brengdahl, J., Engberg, S., Schwinn, M.K., Slater, M.R., Lundin, A., Hsieh, P.P., Li, S., et al. (2023). Simultaneous inhibition of DNA-PK and Polθ improves integration efficiency and precision of genome editing. *Nat. Commun.* **14**, 4761.
15. Renaud, J.-B., Boix, C., Charpentier, M., De Cian, A., Cochenne, J., Duvernois-Berthet, E., Perrouault, L., Tesson, L., Edouard, J., Thinard, R., et al. (2016). Improved Genome Editing Efficiency and Flexibility Using Modified Oligonucleotides with TALEN and CRISPR-Cas9 Nucleases. *Cell Rep.* **14**, 2263–2272.
16. Richardson, C.D., Ray, G.J., DeWitt, M.A., Curie, G.L., and Corn, J.E. (2016). Enhancing homology-directed genome editing by catalytically active and inactive CRISPR-Cas9 using asymmetric donor DNA. *Nat. Biotechnol.* **34**, 339–344.
17. Yumlu, S., Stumm, J., Bashir, S., Dreyer, A.-K., Lisowski, P., Danner, E., Kühn, R., and Wurst, W. (2017). Gene editing and clonal isolation of human induced pluripotent stem cells using CRISPR/Cas9. *Methods* **121–122**, 29–44.
18. Harmsen, T., Klaasen, S., van de Vrugt, H., and te Riele, H. (2018). DNA mismatch repair and oligonucleotide end-protection promote base-pair substitution distal from a CRISPR/Cas9-induced DNA break. *Nucleic Acids Res.* **46**, 2945–2955.
19. Okamoto, S., Amaishi, Y., Maki, I., Enoki, T., and Mineno, J. (2019). Highly efficient genome editing for single-base substitutions using optimized ssODNs with Cas9-RNPs. *Sci. Rep.* **9**, 4811.
20. Acosta, S., Fiore, L., Carota, I.A., and Oliver, G. (2018). Use of two gRNAs for CRISPR/Cas9 improves bi-allelic homologous recombination efficiency in mouse embryonic stem cells. *Genesis* **56**, e23212.
21. Glaser, A., McColl, B., and Vadolas, J. (2016). GFP to BFP Conversion: A Versatile Assay for the Quantification of CRISPR/Cas9-mediated Genome Editing. *Mol. Ther. Nucleic Acids* **5**, e334.
22. Wang, Y., Liu, K.I., Sutrisnoh, N.A.B., Srinivasan, H., Zhang, J., Li, J., Zhang, F., Lalith, C.R.J., Xing, H., Shanmugam, R., et al. (2018). Systematic evaluation of CRISPR-Cas systems reveals design principles for genome editing in human cells. *Genome Biol.* **19**, 62.
23. Karakikes, I., Stillitano, F., Nonnenmacher, M., Tzimas, C., Sanoudou, D., Termlinchan, V., Kong, C.W., Rushing, S., Hansen, J., Ceholski, D., et al. (2015). Correction of human phospholamban R14del mutation associated with cardiomyopathy using targeted nucleases and combination therapy. *Nat. Commun.* **6**, 6955.
24. Feyen, D.A.M., Perea-Gil, I., Maas, R.G.C., Harakalova, M., Gavidia, A.A., Arthur Ataam, J., Wu, T.H., Vink, A., Pei, J., Vadgama, N., et al. (2021). Unfolded Protein Response as a Compensatory Mechanism and Potential Therapeutic Target in PLN R14del Cardiomyopathy. *Circulation* **144**, 382–392.
25. Arthur Ataam, J., Belbachir, N., Perea-Gil, I., Termlinchan, V., Vadgama, N., Garg, P., Ramchandani, R., Gavidia, A.A., Roura, S., Gálvez-Montón, C., et al. (2024). Empagliflozin Attenuates Arrhythmias in an iPSC-Based Model of Hypertrophic Cardiomyopathy. *Circ. Genom. Precis. Med.* **17**, e004526.
26. Perea-Gil, I., Seeger, T., Bruyneel, A.A.N., García-López, E., García-Pérez, V., López-Maderuelo, D., Jiménez-Borreguero, L.J., Díez-Juan, A., Gavidia, A.A., Arthur Ataam, J., et al. (2022). Serine biosynthesis as a novel therapeutic target for dilated cardiomyopathy. *Eur. Heart J.* **43**, 3477–3489.
27. Bruyneel, A.A.N., Colas, A.R., Karakikes, I., and Mercola, M. (2019). AlleleProfileR: A versatile tool to identify and profile sequence variants in edited genomes. *PLoS One* **14**, e0226694.
28. Stillitano, F., Hansen, J., Kong, C.W., Karakikes, I., Funck-Brentano, C., Geng, L., Scott, S., Reynier, S., Wu, M., Valogné, Y., et al. (2017). Modeling susceptibility to drug-induced long QT with a panel of subject-specific induced pluripotent stem cells. *eLife* **6**, e19406.
29. Skarnes, W.C., Pellegrino, E., and McDonough, J.A. (2019). Improving homology-directed repair efficiency in human stem cells. *Methods* **164**, 18–28.